Fourteenth USA/Europe Air Traffic Management Research and Development Seminar (ATM2021)

COVID-19: Passenger Boarding and Disembarkation

Michael Schultz*, Majid Soolaki†, Elnaz Bakhshian††, Mostafa Salari‡, Jörg Fuchte§

*Dresden University of Technology
Insitute of Logistics and Aviation
Dresden, Germany

University College Dublin
† Lochlann Quinn School of Business
†† School of Civil Engineering
Dublin, Ireland

‡University of Calgary
Department of Civil Engineering
Calgary, Canada

§Diehl Aviation
Hamburg, Germany

***Abstract*—Boarding and disembarking an aircraft is a time-critical airport ground handling process. Operations in the confined aircraft cabin must also reduce the potential risk of virus transmission to passengers under current COVID-19 boundary conditions. Passenger boarding will generally be regulated by establishing passenger sequences to reduce the influence of negative interactions between passengers (e.g., congestion in the aisle). This regulation cannot be implemented to the same extent when disembarking at the end of a flight. In our approach, we generate an optimized seat allocation that takes into account both the distance constraints of COVID-19 regulations and groups of passengers traveling together (e.g., families or couples). This seat allocation minimizes the potential transmission risk, while at the same time we calculate improved entry sequences for passengers groups (fast boarding). We show in our simulation environment that boarding and disembarkation times can be significantly reduced even if a physical distance between passenger groups is required. To implement our proposed sequences during real disembarkation, we propose an active information system that incorporates the aircraft cabin lighting system. Thus, the lights above each group member could be turned on when that passenger group is requested to disembark.**

***Keywords*—Passenger disembarkation, virus transmission, COVID-19, pandemic requirements, passenger groups in aircraft cabin, two-objective mathematical modeling**

I. Introduction

The COVID-19 situation will have a lasting impact on air transportation in general and on airport operations (aircraft handling) and passenger handling in particular. The current pandemic situation requires two major changes to normal aircraft handling procedures: (a) passengers must maintain a certain distance when boarding and disembarking, and (b) in addition to normal cleaning procedures, the aircraft cabin must be disinfected to avoid potential virus transmission via surface contact. Fig. 1 illustrates that the required process changes will have a significant impact on aircraft turnaround time, as these processes are part of the critical operating path. Studies that consider COVID-19 constraints for passenger boarding [1] and aircraft cleaning [2] highlight the need for appropriate process adjustments to mitigate the impact of significantly increased process times. However, there has not yet been an intensive scientific discussion of passenger disembarkation sequences under COVID-19 conditions [3].

There are several approaches to infrastructural changes in the aircraft cabin to reduce transmission risks, but most of these ideas are far from being a flexible and standardized solution for the aviation industry. From an operational perspective, adapted boarding strategies are more likely to be put into practice by airlines and airports than modified cabin equipment. Disembarkation is more difficult to control by regulation, and passengers show poor discipline and limited willingness to behave in a compliant manner while disembarking from the aircraft. This is particularly noteworthy because the risk of virus transmission is much higher during uncontrolled disembarkation than during controlled boarding of the aircraft [4].

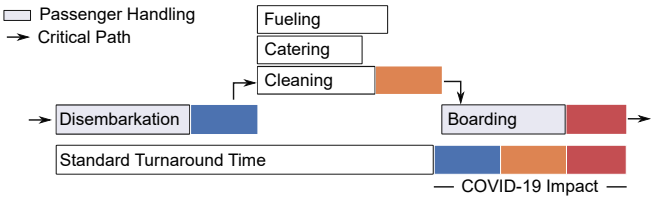

Figure 1: Impact of COVID-19 regulations on aircraft turnaround operations, in particular during disembarkation, cleaning, boarding.

In our approach, we assume that passengers travel in groups and that boarding and disembarkation could be controlled by the present technical infrastructure. The idea behind considering group constellations is that group members, in the form of families or couples, were already in close contact with each other before entering the aircraft and should not be subject to spatial spacing rules. While we propose a standard call-in procedure for boarding, we assume that groups of passengers can be instructed to stand up and leave the aircraft through the seat-based lighting system of the aircraft cabin. In addition, passengers will initially be responsible for maintaining a minimum distance from other groups themselves, with cabin crew monitoring this process. In a later phase, this may also be supported by new technologies for precise passenger location and the associated automated monitoring and control of passenger movements via personal devices (see Fig. 2).

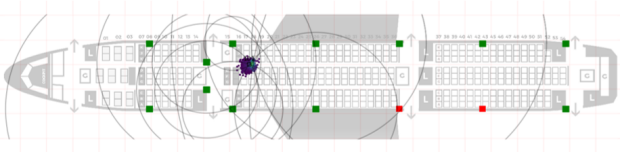

Figure 2: Estimation of passenger position based on localization framework in a digital connected cabin using stationary anchors (red and green circles) and signals from mobile devices [5].

Aircraft cabins have difficult conditions for wireless signals due to possible reflections, scattering and attenuation of transmitted signals. In this context, ultra-wideband (UWB) technology will enable precise, real-time localization for indoor applications and could provide reliable range measurements for compliance to COVID-19 regulations [5]. UWB is already being integrated into personal devices for the consumer market. In the context of future passenger handling in the confined aircraft environment, an efficient sensing environment will be a key element for improved situational awareness of system conditions (e.g., aisle occupancy or baggage compartment status). This information can be used to further improve operational efficiency and enable new product developments and passenger-oriented services.

A. Review of state of the art

Comprehensive overviews are provided for passenger boarding research [6–8] and aircraft ground operations [9]. Only a few aircraft boarding and disembarkation tests have been conducted to provide data for the calibration of input parameters and validation of simulation results: using a mock Boeing 757 fuselage [10], time to store hand luggage items in the overhead compartments [11], small-scale laboratory tests [12], evaluation of passenger perceptions during boarding and disembarkation [13], operational data and passenger data from field trial measurements [14], field trials for real-time seat allocation in connected aircraft cabin [15], and using a B737-800 mock-up (1/3 size) to explore the factors affecting the time of luggage storage [16]. Although these field data are used for simulation experiments, they only cover regular behavior in a pre-pandemic situation.

The particular movement behavior of pedestrians depends significantly on group constellations (e.g. friends or families) and impacts the self-organization capabilities of crowds [17–19]. Also in the context of passenger dynamics in the airport, it is an important fact that up to 70% of the tourists and 30% of the business passengers are traveling in groups [20]. Thus, group constellations are important to understand granular flow patterns during boarding and disembarkation (e.g. couples or families are not separated). Group behavior may shorten the process times since conflicts during the seating process are internally solved [21] and aircraft boarding by rows should be a recommended practice [11]. An approach of dynamically optimized boarding indicates that the boarding process benefits from the consideration of groups [22]. Furthermore, less complex boarding sequences (e.g. random or block boarding) benefit more from the consideration of passenger groups (approx. 5% faster boarding), while seat-based sequences (separation of the window, middle, and aisle seats) lead to longer boarding times [6].

While passenger boarding research exhibits a broad range of improvements (e.g. group boarding, sequence optimization, infrastructural changes), research in the specific field of passenger disembarkation is quite limited and findings often arise as a side product. Two general concepts are addressed to analyze the efficacy of block-wise (aggregated seat rows) or column-wise (e.g. all aisle seats) sequences. Here, column-wise disembarkation was found to be more effective for narrow-body aircraft [23]. These two structured disembarkation sequences are analyzed in small-scale field trials applying inside-out (column-wise) and back-to-front (block-wise) sequences [24], but in contrast to the prior simulation experiment [25], no significant improvements of the disembarkation time could be demonstrated.

Currently, the research focus is set on efficient passenger handling in the aircraft cabin during pandemic situations. Standard boarding sequences are analyzed considering the quantity and quality of passenger interactions and evaluated with a virus transmission model to provide a more detailed assessment. The implementation of physical distances indicates that conventional boarding sequences take longer and trade-offs between economic efficiency (seat load) and process duration must be made to minimize the impact on various health risks [26]. Adjusted seat allocation sequences are developed considering both distances to the aisle (ensure lower transmission risks caused by aisle movements) and distance between the occupied seats [27]. Furthermore, investigation shows that physical distances between passengers decrease the number of possible transmissions by approx. 75% for random boarding sequences, and could further decreased by more strict reduction of hand luggage items (less time for storage, compartment space is always available) [4]. Furthermore, standard process times could be reached if the rear aircraft door is used for boarding and disembarkation. This investigation also points out that disembarkation consists of the highest transmission potential and only minor benefits from distance rules and hand luggage regulations. The optimized consideration of passenger groups in the context of a pandemic boarding scenario will significantly contribute to a faster process (reduction of time by about 60%) and a reduced transmission risk (reduced by 85%), which reaches the level of boarding times in pre-pandemic scenarios [1]. The results of the passenger process evaluation considering the current COVID-19 situation were taken as input to further investigate the impact of pandemic requirements on the aircraft turnaround [2]. Here an integrated cleaning and disinfection procedure was developed and optimized. Under COVID-19 constraints, aircraft turnarounds require between 10% (with additional personnel) and 20% (without additional personnel) more ground time. Finally, aircraft disembarkation has not yet been properly addressed and is missing to complete the picture of operational impacts of COVID-19 [3].

B. Focus and structure of document

We provide in our contribution an approach for aircraft boarding and disembarkation considering a physical distance between groups of passengers (e.g. families or couples). In previously conducted research, it was already shown that the consideration of passenger groups shorten boarding time. The paper is structured as follows. After the introduction (Section I), we briefly introduce a stochastic cellular automaton approach, which is used for modeling the passenger movements in the aircraft cabin (Section II). A transmission model is implemented to evaluate the virus transmission risk during passenger movements. In Section III, we motivate and introduce a problem description to derive optimized sequences of

passenger groups during boarding. This approach is extended in Section IV to allows weighting disembarkation time and a transmission risk indicator in the objective function. This sequence is then implemented in the cellular automaton model to verify the results. Finally, we conclude our research with a summary and an outlook (Section V).

II. Model for passenger movement in the cabin

The individual movement behavior of passengers in the aircraft cabin is modeled by a cellular automaton approach [6], which covers short (e.g. avoid collisions, group behavior) and long-range interactions (e.g. tactical wayfinding). This cellular automaton model is based on an individual transition matrix, which contains transition probabilities to move to adjacent positions around the current passenger position [28].

A. Operational constraints and rules of movement

The implemented cellular automaton model considers operational conditions of aircraft and airlines (e.g. seat load factor, conformance to the boarding procedure) as well as the non-deterministic nature of the underlying passenger processes (e.g. hand luggage storage) and was calibrated with data from the field [14]. The cellular automaton for aircraft boarding and disembarkation is based on a regular grid (Fig. 3), which consists of equal cells with a size of 0.4 x 0.4 m, where a cell can either be empty or contain exactly one passenger. Passengers can only move one cell per timestep or must stop if the cell in the direction of movement is occupied.

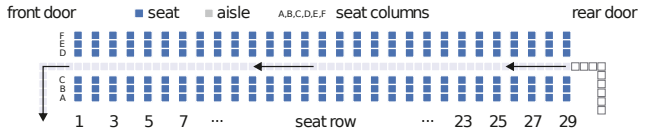

Figure 3: Grid-based aircraft model with 29 seat rows and 6 seats per row (reference layout for single-aisle, narrow-body configurations). Layout shows one door in use for disembarkation.

The boarding progress consists of a simple set of rules for the passenger movement: (a) enter the aircraft at the assigned door (based on the current boarding scenario), (b) move forward from cell to cell along the aisle until reaching the assigned seat row, and (c) store the luggage (aisle is blocked for other passengers) and take the seat. The storage time for the hand luggage depends on the individual number of hand luggage items. The seating process depends on the constellation of already used seats in the corresponding row. The agents are sequenced concerning the active boarding sequence. From this sequence, a given percentage of agents are taken out of the sequence (non-conforming behavior) and inserted into a position, which contradicts the current sequence (e.g. inserted into a different boarding block).

For the disembarkation the movement rules are: (a) all passengers are seated in the aircraft according to an initial seat configuration, (b) passengers could enter the aisle if the seats at their corresponding row are free and the aisle is not blocked by other passengers, (c) if passengers enter the aisle, they take their hand luggage items out of the overhead compartment and block the corresponding aisle cell, (d) if all hand luggage items are taken, passengers move in the direction of the assigned aircraft door by entering empty aisle cells in front of them.

The maximum, free walking speed in the aisle is 0.8 m/s [15], so a simulation timestep is 0.5 s. In each simulation step, the list of passengers to be updated is randomly shuffled to emulate a parallel update behavior for the discrete time dynamics (random-sequential update) [28, 29]. Each boarding and disembarkation scenario is simulated 125,000 times, to achieve statistically relevant results defined by the average boarding/disembarkation time. Further details regarding the general model, parameter setups, and the simulation environment are provided in [6].

For the COVID-19 scenarios, an additional assumption is that a cell is blocked if entering or moving in the aisle would violate the separation distance between passengers or groups of passengers (e.g., families or couples). In the context of physical separation, the International Aviation Transport Association (IATA) requires a minimum separation distance of 1 m [30] and the Federal Aviation Administration (FAA) requires a minimum separation distance of 6 feet (2 meters) [31]. Considering the cellular automaton model with its regular grid structure (cell spacing of 0.4 m) and to maintain comparability with our previous results [1, 2, 4], the minimum physical spacing was set at 1.6 m (4 cells). At this point, we assume that passengers are informed that a distance of 1.6 m corresponds to the distance between 2 rows of seats, which provides sufficient visual orientation for the passengers.

B. Transmission model

The basic cellular automaton developed for stochastic passenger movements is extended to include an approach for assessing the risk of virus transmission during boarding and disembarkation. Transmission risk can be defined by two main factors: Proximity to the index case and duration of contact time. A simplified approach is to count both the individual interactions (passengers in adjacent cells) and the duration of these contacts in the aisle and during the seating process. However, counting individual contacts provides only an initial indication of possible ways of infection. Our approach is based on a transmission model [32], which defines the spread of SARS-CoV2 coronavirus as a function of distance, using different distance measures [33]. Here, the probability of a person n being infected by a person m is described by (1).

$$P_n = 1 - exp\left(-\theta \sum_m \sum_t \mathrm{SR}_{m,t} \quad i_{nm,t} \quad t_{nm,t}\right) \tag{1}$$

defined by:

- P_n Probability of person n to receive an infectious dose. Not “infection probability”, which depends highly on the immune response of the affected person.
- θ Calibration factor for the specific disease.
- $\mathrm{SR}_{m,t}$ Shedding rate, the amount of virus the person m spreads during the timestep t.
- $i_{nm,t}$ Intensity of the contact between n and m during the timestep t, which corresponds to their distance.
- $t_{nm,t}$ Time person n interacts with person m at timestep t.

Considering this idea, we define the shedding rate *SR* as a normalized bell-shaped function (2) with $z \in (x, y)$ for both longitudinal and lateral dimensions, respectively. The parameters are a (scaling factor), b (slope of leading and falling edge), and c (offset) to determine curve shape.

$$\mathrm{SR}_{xy} = \prod_{z \in (x,y)} \left(1 + \frac{|z - c_z|^{2b_z}}{a_z} \right)^{-1} \tag{2}$$

SR was calibrated in a prior study [4] based on the transmission events of an actual flight [34]. We have applied the corresponding parameter setting with $a_x = 0.6$, $b_x = 2.5$, $c_x = 0.25$, $a_y = 0.65$, $b_y = 2.7$, and $c_y = 0$. This causes the footprint in the y-direction (lateral to the direction of motion) to be smaller than in the x-direction (in the direction of motion). When passengers reach their seat row and start to store the hand luggage or enter the seat row, the direction of movement is changed by 90°, heading to the aircraft window.

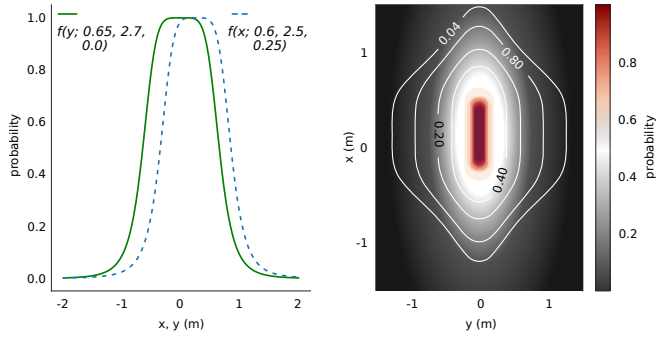

Figure 4: Transmission probability for longitudinal x and lateral y components (left), and (x,y) probability field (right) [1].

Finally, the individual probability for virus transmission P_n corresponds to Θ, the specific intensity per timestep (3).

$$P_n = \Theta \ \mathrm{SR}_{xy} \ \alpha \tag{3}$$

In accordance with [4], Θ is set to $\frac{1}{20}$, which means a passenger reaches a probability of $P_n = 1$ after standing 20 s in closest distance in front of an infected passenger ($\mathrm{SR}_{xy} = 1$). The parameter $\alpha \in \{1, 2\}$ is 1 and changed to 2 when the passenger stores the luggage or enters the seat row. This doubled shedding rate reflects the higher physical activities within a short distance to surrounding passengers.

III. Passenger Boarding

A. Nominal case - single passengers

We introduce a baseline setup to depict the results for the evaluation of transmission risks [6]. Table I shows the comprehensive evaluation of transmissions around one infected passenger, which is randomly seated in the aircraft cabin. Two different scenarios are evaluated against the reference implementation (R) of the boarding strategies: (A) applying a minimum physical distance between two passengers of 1.6 m, and (B) additionally to the physical distance, the number of hand luggage items is reduced by 50% (implemented by reducing the storing time by 50%). Scenarios A and B are additionally extended by the use of two aircraft doors (one in the front and at the rear) during boarding, scenarios A2 and B2. The transmission risk and the boarding time are used as evaluation criteria [4]. The analysis points out that, in particular, the back-to-front sequence (2 blocks: front block with rows 1-15, rear block with rows 16-29) exhibits lower values for the transmission probability than the optimized block sequence (using 6 blocks of aggregated seat rows) (see [6]). When passengers board (block-wise) from the back to the front, the chance to pass an infected person is reduced to a minimum, which is confirmed by the reduced transmission probability exhibited in Table I. This effect is also a root cause of the low transmission risks of the outside-in, reverse pyramid, and individual boarding sequence.

TABLE I. Transmission risk assessment assuming a SARS-CoV2 passenger in the cabin, graded by four categories: random, block-based, row- and individual-based, and disembarkation.

boarding strategies: boarding sequence	R	A	B	A2	B2	R	A	B	A2	B2
	Transmission risk (a.u.)					Boarding time (%)				
Random	5.9	1.6	1.1	1.4	1.0	100	198	154	133	103
Back-to-front (2 blocks)	5.6	1.4	1.0	1.2	0.8	96	220	169	153	116
Optimized block (6 blocks)	6.5	2.3	1.5	1.5	1.0	95	279	210	166	125
Outside-in	3.5	0.4	0.2	0.3	0.1	80	161	116	107	77
Reverse pyramid	3.0	0.2	0.1	0.2	0.1	75	185	128	119	82
Individual	2.0	0.2	0.1	0.2	0.1	66	114	104	103	74
Disembarkation	10.0	9.7	7.8	7.6	6.0	55	97	68	52	36

The use of two aircraft doors for boarding will provide an appropriate solution for a reduced transmission risk inside and outside the cabin, if near apron stands could be used and passengers could walk from the terminal to the aircraft. This kind of *walk boarding* also prevents passengers from standing in the badly ventilated jetway during the boarding. Disembarkation is difficult to control by specific procedures given that passengers demonstrated little discipline and high eagerness to leave the aircraft. More attention should be paid to this process and consideration should also be given to procedural or technical solutions to provide passengers better guidance and control.

B. Passenger Groups

We consider passenger groups as an important factor to derive an appropriate seat allocation and boarding sequence. The main idea behind the group approach is that members of one group are allowed to be close to each other, as they are already in close contact with each other before boarding, while different groups should be separated as far apart as necessary.

We develop a mathematical model to determine an optimal strategy for assigning seats in the cabin under the objective to minimize the virus transmission risk. The idea to create an appropriate seat allocation for a pandemic situation includes three assumptions. The first one is that an airline could assign just a percentage of the available seats (e.g. 50%) to reduce the virus transmissions in the cabin and this strategy will be the primary solution to face the pandemic situation. The next assumption is about minimizing passenger contacts or maximizing the distances between passengers in the cabin

and guaranteeing at the same time that the confined space inside the aircraft is used efficiently.

Although complex boarding sequences, such as outside-in, reverse pyramid, and individual lead to better boarding times, there will be an issue. The boarding process is driven by the willingness of passengers to follow the proposed strategy. We will assume a group of four members (e.g. a family) to be seated. If one of these boarding strategies is applied, they will have just two options. The first one is seating near each other, therefore they have to split during the boarding. The next option is remaining as one group in the boarding sequence and as a result, they have to seat in different rows. Both options are inconvenient for group members (families). Here we propose to look at the group members as a community since they were already in close contact before boarding. The strategy that is used in Fig. 5 depicts a general solution, but it could be improved considering groups. Without loss of generality, we could suppose that the transmission rate for the members of each group is zero, which will result in better use of space and create a new pattern.

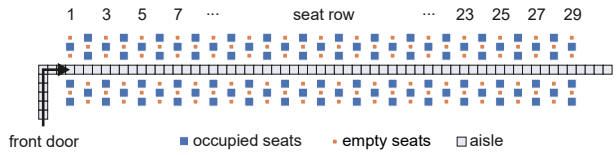

Figure 5: Fifty percent of the seats will be allocated to passengers during the pandemic situation according to a pattern with maximum physical separation.

The introduced concept of a shedding rate of infected passengers will be used here as well. If an infected passenger was assigned to different columns, the several shedding rates must be counted based on the location of the adjacent locations. Taking Fig. 6 as an example, when a passenger seated in row $i = 21$ and column C (aisle), we compute the shedding rate for the passenger from other groups that seat in the same row ($i = 21$ at column A (window), B (middle), and D (aisle)) and previous row $i - 1 = 20$ (column B (middle), C (aisle), and D (aisle)).

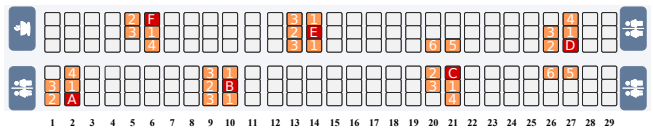

Figure 6: Types of passenger interactions (orange) in the aircraft cabin around the infected passengers (red) considering different seat positions: besides (1 and 4), in front (2), diagonally in front (3), and across the aisle (5 and 6).

Based on the assumptions of the problem description, we set up an optimization model [1]. We tried to solve the mathematical model for a medium-size problem (e.g. 10 groups, 10 seat rows) but the run time increased significantly and the optimization software (GAMS with CPLEX solver) could not find an optimal solution in a reasonable time (10 hours). Therefore, we designed a Genetic Algorithm (GA) for the real-sized problem. The problems run on a computer with AMD Ryzen 7, 3700U, 2.30GHz CPU, 16 GB RAM, and Matlab 2013 software is used for running the GA. We choose six scenarios for the optimization and used the optimal seat allocation in the passenger boarding simulation to derive an appropriate boarding sequence with a low transmission risk.

The corresponding solutions for the three scenarios with a 50% seat load (87 passengers) are illustrated in Fig. 7. The values of the objective function (O.F.) of these three scenarios indicate that our approach (scenario 3) for an improved seat allocation should also result in a significant reduction of the transmission risk: a reduction of 91% of O.F. value compared to scenario 1 (seats are assigned randomly to passengers with a maximum distance), and a reduction of 85% compared to scenario 2 (seats are assigned randomly, group members in the same zone). The implementation of the mixed-integer

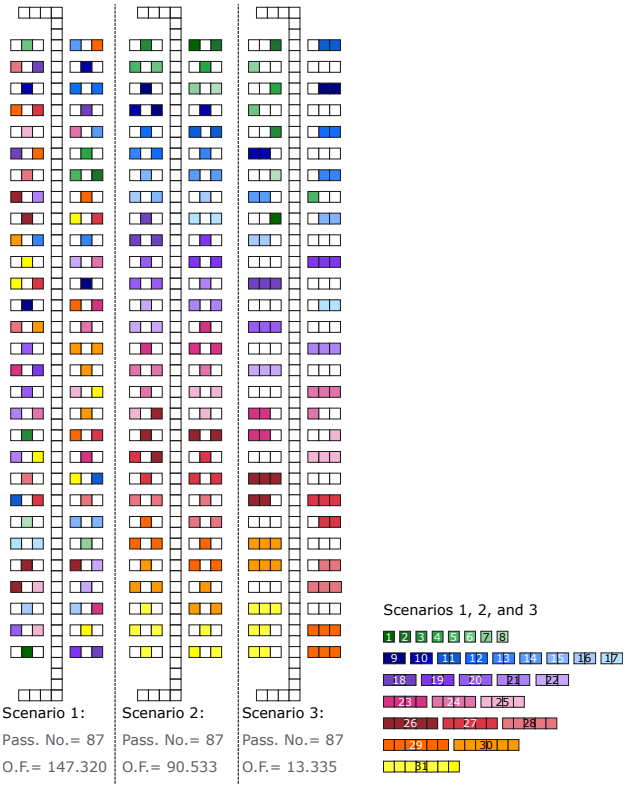

Figure 7: Seat allocation in the aircraft cabin considering 87 passengers (31 groups) assigned to different groups using regular pattern (scenario 1 and 2) and improved group-based seat allocation (scenario 3).

linear programming model and the genetic algorithm leads to an improved allocation for the passengers to be seated in the aircraft cabin. This seat allocation is used as input for the passenger boarding model, which was extended by a transmission module to evaluate transmission risk during aircraft boarding, to derive an optimum sequence to board the passengers.

Analyses in the context of appropriate boarding sequence accompanied by the introduction of infrastructural changes showed that an improved sequence comprises a mix of boarding per seat (from window to aisle) and per seat row (from the rear to the front) [35]. First and foremost, per-seat boarding (window seats first) is the most important rule to ensure seating without additional interaction in the seat rows.

Starting with an outer seat in the last row, the number of group members and the necessary physical distance between passengers (1.6 m) defines the subsequently following seat row, which could be used in parallel (e.g. 6 passengers with seat row 29 will block the aisle until seat row 27 (waiting), the physical distance requires to block row 26 and 25, the next group must have seats in front of row 25). This process of seat and row selection is repeated until the front of the aircraft is reached and is repeated until all passengers are seated. We further assume that the passengers in each group will organize themselves appropriately to minimize local interactions.

If the sequencing algorithm is applied to the optimized seat allocation from scenario 3, the passenger groups are boarded in five segments. Inside each group, the distance between passengers is not restricted but between groups, it is constrained by 1.6 m (last member of the first group and the first member of the following group). The first segment starts with group 31 and the last segment with group 14 (see Fig. 8). As an example, the passengers inside group 31 (yellow) are

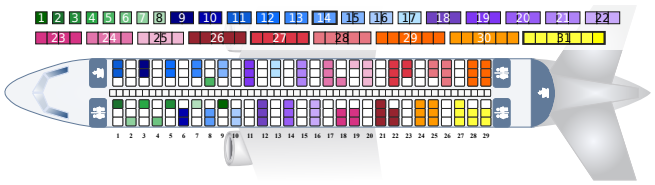

Figure 8: Optimized boarding of 31 groups considering a physical distance of 1.6 m between passengers of different groups.

organized by the following sequence of seats, which results in a minimum of individual seat and row interactions: 29A, 29B, 28A, 28B, 27A, 27B, and 27C. Considering distances between groups, the best candidate will be group 27 (red) with seats 23F, 23E, 22F, 22E, and 22D. This sequence allows both groups to start the seating process in parallel, without waiting time due to a too small distance between the seat rows.

In the three scenarios, 87 passengers are boarded with different sequences (see Fig. 7): individual passengers in a regular pattern (scenario 1), groups in a regular pattern (scenario 2), and groups in an optimized seat allocation (scenario 3). Scenario 1 is used as a reference case to evaluate the performance (boarding time) and the transmission risk of scenarios 2 and 3 (Table II).

TABLE II. Evaluation of average boarding times and transmission risk during boarding assuming a randomly selected contagious passenger at 50% seat occupancy (87 passengers).

Scenario	Sequence	Time (%)	Transmission risk (a.u.)
1	random	100.0	0.58
	best sequence	45.2	0.00
2	groups, random sequence	68.0	0.62
	groups, best sequence	51.9	0.20
3	groups, optimal allocation random sequence	69.0	0.57
	groups, optimal allocation best sequence	**41.1**	**0.09**

Therefore, a passenger sequence is established for both random and individual boarding sequences (optimized). The boarding time for the random sequence is set to 100%, as reference. As shown in Table II, the implementation of the individual sequence will reduce the boarding time to 45.2% at a minimum of transmission risk. The consideration of groups (scenarios 2 and 3) using the random sequence already reduces the boarding time by about a third at a comparable level of transmission risk. If the optimized seat allocation is used together with the individual groups the boarding time could be further reduced to 41.1% at a low transmission risk of 0.09 new infected passengers on average (85% reduction).

IV. Passenger Disembarkation

While boarding can be controlled to some degree, passenger disembarkation takes place in a less controllable environment. In a first and simplified approach, passenger groups were disembarked in batches of passenger groups. In this case, groups within a batch are allowed to enter the aisle in parallel, while ensuring that the minimum distance between groups is maintained at all times. After a group has been allowed to disembark, all members of the group enter the aisle, take their hand luggage, and wait until the group in front of them begins disembarking. Subsequent groups may begin when the last group in the current batch has passed their row. In future operational scenarios, passenger groups could be notified directly via personal devices or active lights on their seats to begin disembarking.

To show how the time for disembarkation changes, a sensitivity analysis is performed. To do this, a group of passengers from the example case above (Fig. 8) is randomly selected and added to the current disembarkation batch with a certain probability. This probability increases in 10% increments from 0% (one group per batch) to 100% (all groups in one batch). In addition, three levels for hand luggage amount are considered: 100% (standard), 50% (reduced), 0% (no items). The scenario with only one group per batch and no hand luggage is chosen as the reference case. The result of this analysis is shown in Fig. 9 using the average disembarkation times and the associated standard deviations as measurements.

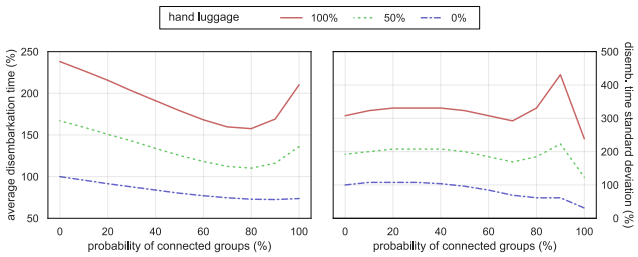

Figure 9: Random group sequence for disembarkation: (a) given probability that the following group is part of the same disembarkation batch, and (b) three level of hand luggage quantity (100% - standard, 50% - reduced, 0% - no items).

The analysis shows that disembarkation will benefit from the superior organization of groups into batches up to a certain point. As a result, average disembarkation times decrease until a minimum is reached at approximately 80%. In general, the standard deviations exhibit also a minimum

in that region (70% - 90%) but show both a significant increasing and decreasing behavior. The reason is that if all passenger groups are in one batch, the disembarkation is a front-to-back process, where groups in the front are leaving the aircraft first. This a somehow a much more stable process than a batch-organized prioritization but also results in higher disembarkation times.

The obtained minimum times indicate a significant potential to reduce the disembarkation time by about 40%. To provide a more improved disembarkation process, a manual assignment of groups will be derived from the introduced seat allocation. Each batch of passenger groups is generated starting with the last occupied seat row. The group of this row will be placed into the aisle, assuming the individual personal space (one cell per passenger). Considering the distance of 1.6 m per group, the nearest group to that location (downstream) is added to the current batch. This process is finished when the first seat row is reached. Fig. 10 exhibits this batch assignment process, where 6 batches are created for the given example. This algorithm-based batch sequence results for the three hand luggage scenarios in reduced disembarkation times by 7%, 27%, and 35% for the zero luggage, 50%, and 100% hand luggage items accordingly (referring to the corresponding minimum times presented at Fig. 9).

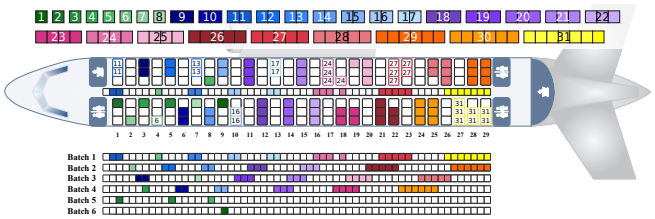

Figure 10: General, batch-oriented disembarkation considering a minimum distance of 1.6 m between passenger groups. The current aisle status corresponds to the first batch of passenger groups ready for disembarkation. The following batches are depicted below.

These results lead to the question of how this process can be further improved. In the following section, we develop a two-objective mathematical model, which includes an optimized disembarkation strategy incorporating passenger groups and physical distance requirements from the current COVID-19 situation. In the development, we are not considering hand luggage items assuming that the average pick-up process will not influence the sequence generation.

The concept of the shedding rates is now used for the disembarkation process. Here, the corresponding shedding rate depends on the position of the infected passenger in the aisle and the positions of the passengers of other groups that will leave their seats afterward. We calculate the transmission risk function for all passengers based on the locations of other passengers. Three types of passenger interference are implemented in our approach. The first type is defined based on the concept of physical distancing. We suppose a close distance between members of each group in the aisle. According to the COVID-19 regulations a physical distance of 1.6 m between groups is implemented (see Fig. 11, part 1).

The second type of interference considers the concept of shedding rates. If an infected passenger leaves the seat, corresponding shedding rates must be calculated based on the location of the other group members who will leave the aircraft after that passenger. Fig. 11 (part 2) demonstrates the interference generated in the two middle rows ($i = 15$ and $i = 16$) when the first member of group 30 (coded orange) is walking in the aisle at period h, where the shedding rates for the passengers from other groups that seat in the related row ($i = 15$ at column D (aisle), E (middle), and F (window)) are calculated. Similarly, the third member of this group could generate different types of interactions for passengers who seat in the next row at the same time ($i = 16$ at column C (aisle), B (middle), and A (window)).

As a result, if the passengers of the first group leave the aircraft earlier, the transmission risk which is the sum of shedding rates of all passengers could be minimized. On the other hand, this strategy leads to longer disembarkation time. Therefore, we have proposed a two-objective mathematical model to handle these two conflicting objectives. The third type of interference is the scheduling process. Taking Fig. 11 (part 3) as an example, if the first member of group 31 arrives in the nineteenth row ($i = 19$) in four seconds then, the passenger who seated in this row and in column F (window) could not leave the seat at that moment. The following assumptions are based on the different types of interference and considering general disembarkation procedures.

- Group members leave their seats at the same time.
- Members of two different groups sitting in a close zone have a certain time interval (e.g. three timesteps) to leave their seats. This distance increases with the number of group members.
- The length of the cabin aisle is 23.2 m.
- The transmission rates are calculated for all passengers.
- Passengers can only leave seats and enter the aisle if this does not result in interference with other passengers.

A. Mathematical model

The following sets, parameters, and decision variables are used in the optimization model.

Notation	**Definition**
Sets and Indexes	
i	Index set of row $i \in \{1, 2, \ldots, \mathcal{I}\}$
k	Index set of passenger group $k \in \{1, 2, \ldots, \mathcal{K}\}$
j	Index set of seat column $j \in \{1, 2, \ldots, \mathcal{J}\}$
h	Index set of time period $h \in \{1, 2, \ldots, \mathcal{H}\}$
r	Index set of interaction type $r \in \{1, 2, \ldots, \mathcal{R}\}$
Parameters	
T_k	Group number k
SR'_j	Related shedding rate for interaction j or r, considering 6 different types based on the number of columns
λ_{ij}	Disembarkation time (in period unit) required for a passenger, seats in row i and column j
Y_{ij}	Binary parameter, equals k if a passenger from group k, seated in in row i and column j; equals zero otherwise
$M_{kk'}$	Binary parameter, equals one if the members of group number k and k' could not leave their seats at the same time (because they will block each other such as groups 30 and 31), equals zero otherwise
w_1	Coefficient weight of the first objective function $w_1 \in [0, 1]$
w_2	Coefficient weight of the second objective function which is equals to $1 - w_1$

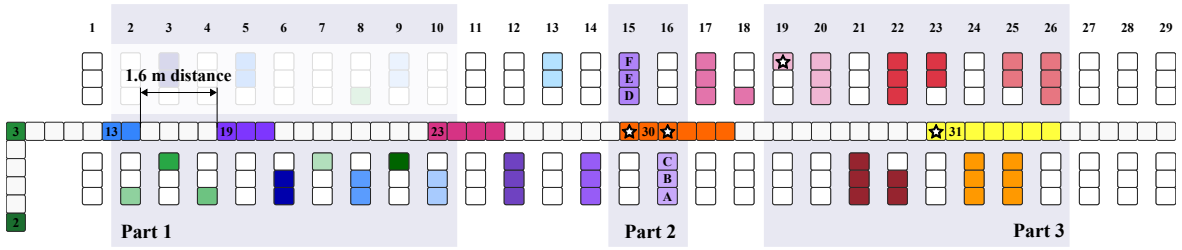

Figure 11: Different types of interference between passengers in the aircraft: physical distance between groups (part 1), close interactions covered by particular shedding rates (part 2, cf. Fig. 6), far-reaching interactions (passenger in row 19 have to wait for group 31 (part 3)).

Notation	**Definition**
Decision Variables	
p_{kh}	Number of members of group k that leave their seats at time period h
x_{ijkh}	Binary variable, equals one if a passenger from group k who is seated in a seat in row i and and column j leaves its seat at the time period h (activation time); equals zero otherwise
q_{ijkh}	Period of time from the moment when a passenger from group k in row i, column j leaves the cabin
$n_{iji'}$	Period of time at the moment when a passenger who has seated in row i, column j reaches row i'
$u_{kk'hh'}$	Binary variable, equals one if group k and k' leave their seats at time period h and h', respectively
z_1	First objective function: disembarkation time
z_2	Second objective function: transmission risk
TZ	Total objective function which is calculated based on two conflicted objectives z

The proposed new multi-objective minimization model for the problem is introduced as follows.

$$\text{TZ} = w_1\left(\frac{z_1 - {z_1}^*}{{z_1}^*}\right) + w_2\left(\frac{z_2 - {z_2}^*}{{z_2}^*}\right) \tag{4}$$

Disembarkation Time:

$$z_1 = \underset{i\in\mathcal{I}, j\in\mathcal{J}, k\in\mathcal{K}, h\in\mathcal{H}}{Max} \; q_{ijkh} \tag{5}$$

Transmission Risk Indicator:

$$z_2 = \sum_{i=1}^{\mathcal{I}}\sum_{j=1}^{\mathcal{J}}\sum_{\substack{k=1\\k=Y_{ij}}}^{\mathcal{K}}\sum_{h=1}^{\mathcal{H}}\sum_{i'=i}^{\mathcal{I}}\sum_{j'=1}^{\mathcal{J}}\sum_{\substack{k'=1\\k'=Y_{i'j'}}}^{\mathcal{K}}\sum_{\substack{h'=1\\h'<h-n_{i'j'i}}}^{\mathcal{H}} {\text{SR}}_j^{'} u_{kk'hh'} \tag{6}$$

The $L-1$ metric method is used to solve the multi-objective decision problem. Therefore, we run the model three times. The first time, we minimize the average disembarkation time, with (5) as an objective function, considering constraints (7)-(16). Thus, the first solution z_1^* could be obtained. Similarly, we minimize the problem concerning minimum transmission risk (6), obtaining the second solution z_2^*. In the third step, we put these two solutions into the general problem, minimize equation (4) under constraints (5)-(16). Here we consider two implementation weights (w_1, w_2) for competing objectives evaluated and set by decision-makers.

$$\sum_{i=1}^{\mathcal{I}}\sum_{j=1}^{\mathcal{J}}\left(\frac{x_{ijkh}}{T_k}\right) + \sum_{i=1}^{\mathcal{I}}\sum_{j=1}^{\mathcal{J}}\sum_{h'=h}^{h+T_k+3}\left(\frac{x_{ijk'h'}}{T_{k'}}\right) \le 1\,, \quad \forall h,k,k', M_{kk'} = 1 \tag{7}$$

$$0.4\sum_{i=1}^{\mathcal{I}}\sum_{j=1}^{\mathcal{J}}\sum_{k=1}^{\mathcal{K}}\sum_{\substack{h'=1\\h'>h-\lambda_{ij}}}^{h} x_{ijkh'} + 1.6\sum_{i'=1}^{\mathcal{I}}\sum_{j'=1}^{\mathcal{J}}\sum_{k'=1}^{\mathcal{K}}\sum_{\substack{h'=1\\h'>h-\lambda_{i'j'}}}^{h}\left(\frac{x_{i'j'k'h'}}{T_{k'}}\right) \le 23.2\,, \quad \forall h > 1 \tag{8}$$

$$\sum_{i=1}^{\mathcal{I}}\sum_{j=1}^{\mathcal{J}} x_{ijkh} = p_{kh}\,, \quad \forall k,h \tag{9}$$

Constraint (7) guarantees that in each timestep two groups sitting in a nearby zone cannot leave their seats at the same time. The physical distances between the passengers in the aisle are determined by constraint (8). A distance of 0.4 m between members of a group and 1.6 m between groups in the aisle is considered. Constraint (9) determines the number of members of each group that leave their place in each period.

$$\sum_{h=1}^{\mathcal{H}} x_{ijkh} = 1\,, \quad \forall i,j,k = Y_{ij} \tag{10}$$

$$T_k x_{ijkh} \le \sum_{i'=1}^{\mathcal{I}}\sum_{j'=1}^{\mathcal{J}} x_{i'j'kh}\,, \quad \forall i,j,k,h \tag{11}$$

$$p_{kh} + p_{k'h'} - 1 \le u_{kk'hh'}\,, \quad \forall k,k',h,h' \tag{12}$$

$$q_{ijkh} \ge h + \lambda_{ij} + 500(x_{ijkh} - 1)\,, \quad \forall i,j,k,h \tag{13}$$

$$q_{ijkh} \le 500 x_{ijkh}\,, \quad \forall i,j,k,h \tag{14}$$

In addition, constraints (10)-(11) guarantee that all members of each group leave their place in the same period. To calculate the decision variables for the shedding rates of two different groups, we define the constraint (12), which is implemented in the transmission risk function. The constraints (13)-(14) represent the disembarkation time of each passenger in each group sitting in row i and column j, and the corresponding decision variable takes the value of zero if the seat was not occupied.

$$n_{iji'} = \lambda_{ij} - i' + h\,, \quad \forall i,j,k = Y_{ij}, h, x_{ijkh} = 1 \tag{15}$$

$$x_{i'j'k'h'} \le |h' - n_{iji'}|\,, \quad \forall i,i',j,j',h',k = Y_{ij}, k' = Y_{i'j'}, k \ne k' > 0 \tag{16}$$

$$x_{ijkh}, u_{kk'hh'} \in \{0,1\}, \quad q_{ijkh}, n_{iji'}, p_{kh}, z_1, z_2 \ge 0\,, \quad \forall i,i',j,k,k',h,h' \tag{17}$$

The third type of interference is formulated in constraints (15)-(16). For each passenger, the arrival time (i.e., $n_{iji'}$) in the lower row i' is determined by (15). Consequently, passengers in this row are not allowed to leave their seats at this time (16). Constraint (17) represents the requirements on the decision variables.

The proposed mathematical model as a scheduling problem is a type of NP-hard. For our real-size problem, we consider 29 rows, 6 columns, 3 interaction types, 31 groups, and 500 periods of time (or seconds). To solve this problem, we implement a meta-heuristic algorithm and used a genetic algorithm to solve the disembarkation problem (cf. [36, 37]).

B. Optimization results

We already use optimized seat layouts [1] and have developed a new mathematical approach with two opposing objective functions. The first objective function gives the

overall disembarkation time and the second objective function targets the transmission risk indicator. In the following, we present the solutions for four example scenarios.

1) Scenario A1: Minimum disembarkation time with 50% occupancy, 87 passengers on the aircraft, divided into 31 groups. Therefore the coefficient weight of disembarkation time equals one ($w_1 = 1$) and the coefficient weight of the transmission risk is supposed to be zero ($w_2 = 0$). The optimized disembarkation progress is shown in Fig. 12. The disembarkation time for the first scenario is 139 s and the transmission risk indicator (second objective function) is calculated in the value of 480.

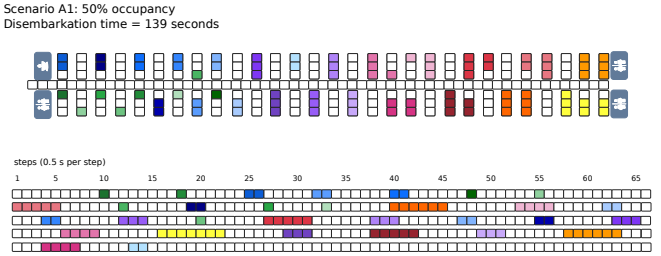

Figure 12: Disembarkation progress for scenario A1, 87 passengers.

2) Scenario A2: Minimum transmission risk with 50% occupancy, 87 passengers (31 groups), $w_1 = 0$, and $w_2 = 1$. Compared to scenario A1, the transmission risk value decreases from 480 to 30 but the disembarkation time increases by 50% (209 s). Scenario A2 was created only for a general comparison of the fitness functions. In the following, only the disembarkation time shall be minimized.

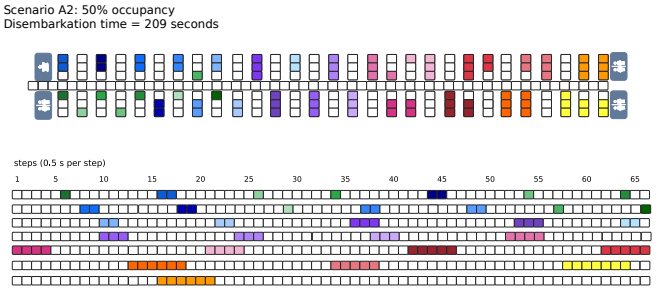

Figure 13: Disembarkation progress for scenario A2, 87 passengers.

3) Scenario B: Minimum disembarkation time with 66% occupancy, 116 passengers on the aircraft, divided into 38 groups. Therefore, the coefficient of the first objective function is supposed to be one. Fig. 14 shows the disembarkation progress with a disembarkation time of 188 s.

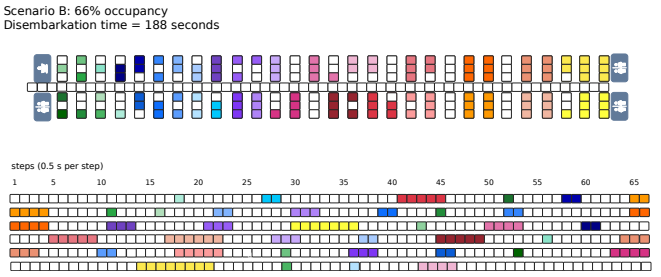

Figure 14: Disembarkation progress for scenario B, 116 passengers.

4) Scenario C: Minimum disembarkation time with 66% occupancy, 174 passengers on the aircraft, divided into 62 groups. Fig. 15 shows the corresponding seat allocation and indicates a disembarkation time of 299 s.

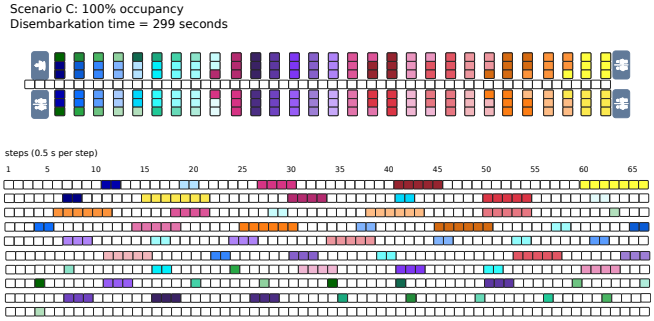

Figure 15: Disembarkation progress for scenario C, 174 passengers.

C. Evaluation of disembarkation process

We must emphasize at this point that we assume each passenger leaves the cabin immediately after entering the aisle. As shown in the exemplary solutions presented (Figs. 12-15), we assume a forward ordered-sequential update of the passenger positions [38]. Thus, the update of positions starts with the passenger closest to the exit (front door), and the positions of subsequent passengers along the aisle are updated next. This approach results in the passenger in the position ahead of the current passenger (in the direction of movement) always moving first, and the exit time is too optimistic. Against this background, we implemented the optimized group sequences in the calibrated stochastic simulation environment to check the disembarkation times. Each group is activated to disembark when the group immediately ahead of it in the disembarkation sequence passes its seat row. This minimizes the potential time/space buffers between group calls as would be required in later operational implementation. Group members enter the aisle only when the physical spacing between groups is assured. Table III summarizes the simulation results.

Scenario	Seat load (%)	Passengers	Disembarkation time (s)		
			Update behavior		
			Forward-ordered	Random	Reference
A1	50	87	139	163	286
B	66	116	188	219	377
C	100	174	299	331	571

TABLE III. Disembarkation of passenger groups considering three scenarios with different seat load factors.

As expected, the result of implementing the forward ordered-sequential update underestimates the disembarkation times by about 30 s. To show the potential for improving the disembarkation time, we use reference cases for each scenario. These reference cases consider the same number of passengers, no groups, no hand luggage items, mandatory physical distance, and realistic random sequential updating behavior. Concerning the reference cases, our optimization

strategy (focusing on a fast disembarkation process) accelerated the process by about 40%.

V. Conclusion and outlook

In the aircraft cabin, passengers must share a confined environment with other passengers during boarding, flight, and disembarkation, which poses a risk for virus transmission and requires risk-appropriate mitigation strategies. Spacing between passenger groups during boarding and disembarkation reduces the risk of transmission, and optimized sequencing of passenger groups helps to significantly reduce boarding and disembarkation time. We considered passenger groups to be an important factor in overall operational efficiency. The basic idea of our concept is that the members of a group should not be separated, since they were already traveling as a group before entering the aircraft. However, to comply with COVID-19 regulations, different passenger groups should be separated spatially. For the particular challenge of disembarkation, we assume that passenger groups will be informed directly when they are allowed to leave for disembarkation. Today, cabin lighting could be used for this information process, but in a future digitally connected cabin, passengers could be informed directly via their personal devices. These devices could also be used to check the required distances between passengers [5]. The implementation of optimized group sequencing has the potential to significantly reduce boarding and disembarkation times, taking into account COVID-19 constraints. In future studies, we will also consider the distribution of carry-on baggage in the cabin. Finally, we intend to further investigate the potential of technical systems that can monitor, evaluate, and, if necessary, regulate passenger boarding and disembarkation.

References

[1] M. Schultz and M. Soolaki, "Analytical approach to solve the problem of aircraft passenger boarding during the coronavirus pandemic," *Transp. Res. Part C: Emerg. Technol.*, vol. 124, p. 102931, 2021.

[2] M. Schultz, J. Evler, E. Asadi, H. Preis, H. Fricke, and C.-L. Wu, "Future aircraft turnaround operations considering post-pandemic requirements," *J. Air Transp. Manag.*, vol. 89, p. 101886, 2020.

[3] C.-Z. Xie, T.-Q. Tang, P.-C. Hu, and H.-J. Huang, "A civil aircraft passenger deplaning model considering patients with severe acute airborne disease," *J. Transp. Saf. Secur.*, pp. 1–22, 2021.

[4] M. Schultz and J. Fuchte, "Evaluation of Aircraft Boarding Scenarios Considering Reduced Transmissions Risks," *Sustainability*, vol. 12, no. 13, p. 5329, 2020.

[5] P. Schwarzbach *et al.*, "Evaluation of Technology-Supported Distance Measuring to Ensure Safe Aircraft Boarding during COVID-19 Pandemic," *Sustainability*, vol. 12, no. 20, p. 8724, 2020.

[6] M. Schultz, "Implementation and application of a stochastic aircraft boarding model," *Transp. Res. Part C Emerg. Technol.*, vol. 90, pp. 334–349, 2018.

[7] C. Delcea, L.-A. Cotfas, and R. Paun, "Agent-Based Evaluation of the Airplane Boarding Strategies' Efficiency and Sustainability," *Sustainability*, vol. 10, no. 6, p. 1879, 2018.

[8] F. Jaehn and S. Neumann, "Airplane boarding," *Eur. J. Oper. Res.*, vol. 244, no. 2, pp. 339–359, 2015.

[9] M. Schmidt, "A review of aircraft turnaround operations and simulations," *Prog. Aerosp. Sci.*, vol. 92, pp. 25–38, 2017.

[10] J. H. Steffen and J. Hotchkiss, "Experimental test of airplane boarding methods," *J. Air Trans. Manag.*, vol. 18, no. 1, pp. 64–67, 2012.

[11] A. Kierzkowski and T. Kisiel, "The Human Factor in the Passenger Boarding Process at the Airport," *Procedia Eng.*, vol. 187, pp. 348–355, 2017.

[12] S. M. V. Gwynne *et al.*, "Small-scale trials on passenger microbehaviours during aircraft boarding and deplaning procedures," *J. Air Transp. Manag.*, vol. 67, pp. 115–133, 2018.

[13] A. Miura and K. Nishinari, "A passenger distribution analysis model for the perceived time of airplane boarding/deboarding, utilizing an ex-Gaussian distribution," *J. Air Trans. Manag.*, vol. 59, pp. 44–49, 2017.

[14] M. Schultz, "Field trial measurements to validate a stochastic aircraft boarding model," *Aerospace*, vol. 5, no. 27, 2018.

[15] ——, "Fast aircraft turnaround enabled by reliable passenger boarding," *Aerospace*, vol. 5, no. 1, p. 8, 2018.

[16] X. Ren, X. Zhou, and X. Xu, "A new model of luggage storage time while boarding an airplane: An experimental test," *J. Air Trans. Manag.*, vol. 84, p. 101761, 2020.

[17] M. Moussaïd, N. Perozo, S. Garnier, D. Helbing, and G. Theraulaz, "The walking behaviour of pedestrian social groups and its impact on crowd dynamics," *PLOS ONE*, vol. 5, no. 4, pp. 1–7, 2010.

[18] M. Schultz, L. Rößger, H. Fricke, and B. Schlag, "Group dynamic behavior and psychometric profiles as substantial driver for pedestrian dynamics," in *Pedestrian and Evacuation Dynamics 2012*, 2013, pp. 1097–1111.

[19] F. Zanlungo, Z. Yücel, and T. Kanda, "Intrinsic group behaviour II: On the dependence of triad spatial dynamics on social and personal features; and on the effect of social interaction on small group dynamics," *PLOS ONE*, vol. 14, no. 12, pp. 1–28, 2019.

[20] M. Schultz and H. Fricke, "Managing passenger handling at airport terminal," in *9th ATM Seminar*, Berlin, 2011.

[21] T.-Q. Tang, S.-P. Yang, H. Ou, L. Chen, and H.-J. Huang, "An aircraft boarding model accounting for group behavior," *J. Air Transp. Manag.*, vol. 69, pp. 182–189, 2018.

[22] H. Zeineddine, "A dynamically optimized aircraft boarding strategy," *J. Air Trans. Manag.*, vol. 58, pp. 144–151, 2017.

[23] A. Wald, M. Harmon, and D. Klabjan, "Structured deplaning via simulation and optimization," *J. Air Transp. Manag.*, vol. 36, pp. 101–109, 2014.

[24] S. Qiang, B. Jia, and Q. Huang, "Evaluation of Airplane Boarding/Deboarding Strategies: A Surrogate Experimental Test," *Symmetry*, vol. 9, no. 10, p. 222, 2017.

[25] S.-J. Qiang *et al.*, "Symmetrical design of strategy-pairs for enplaning and deplaning an airplane," *J. Air Transp. Manag.*, vol. 54, pp. 52–60, 2016.

[26] L.-A. Cotfas, C. Delcea, R. J. Milne, and M. Salari, "Evaluating Classical Airplane Boarding Methods Considering COVID-19 Flying Restrictions," *Symmetry*, vol. 12, no. 7, p. 1087, 2020.

[27] M. Salari, R. J. Milne, C. Delcea, L. Kattan, and L.-A. Cotfas, "Social distancing in airplane seat assignments," *J. Air Transp. Manag.*, vol. 89, p. 101915, 2020.

[28] M. Schultz, "Stochastic transition model for pedestrian dynamics," in *Pedestrian and Evacuation Dynamics 2012*, 2013, pp. 971–985.

[29] ——, "Entwicklung eines individuenbasierten Modells zur Abbildung des Bewegungsverhaltens von Passagieren im Flughafenterminal," PhD thesis, TU Dresden, Dresden, 2010.

[30] International Aviation Transport Association (IATA), "Guidance for cabin operations during and post pandemic, edt. 4," 2020.

[31] Federal Aviation Administration (FAA), "COVID-19: Updated interim occupational health and safety guidance for air carriers and crews," 2020.

[32] T. Smieszek, "A mechanistic model of infection: why duration and intensity of contacts should be included in models of disease spread." *Theor. Biol. Med. Model.*, vol. 6, no. 25, 2009.

[33] S. A. Müller, M. Balmer, A. Neumann, and K. Nagel, "Mobility traces and spreading of covid-19," *medRxiv*, 2020.

[34] S. J. Olsen *et al.*, "Transmission of the severe acute respiratory syndrome on aircraft," *New England Journal of Medicine*, vol. 349, no. 25, pp. 2416–2422, 2003.

[35] M. Schultz, "Dynamic change of aircraft seat condition for fast boarding," *Transp. Res. Part C Emerg. Technol.*, vol. 85, pp. 131–147, 2017.

[36] M. H. L. van den Briel, J. R. Villalobos, G. L. Hogg, T. Lindemann, and A. V. Mulé, "America West Airlines Develops Efficient Boarding Strategies," *INFORMS J. Appl. Anal.*, vol. 35, pp. 191–201, 2005.

[37] M. Soolaki *et al.*, "A new linear programming approach and genetic algorithm for solving airline boarding problem," *Appl. Math. Model.*, vol. 36, pp. 4060–4072, 2012.

[38] A. Schadschneider, D. Chowdhury, and K. Nishinari, "Chapter two - methods for the description of stochastic models," in *Stochastic Transport in Complex Systems*, A. Schadschneider, D. Chowdhury, and K. Nishinari, Eds. Amsterdam: Elsevier, 2011, pp. 27–70.